

A STUDY ON THE AIRLOCK MECHANISM OF THE OIL SUPPLY PUMP IN AERO-ENGINE LUBRICATING OIL SYSTEM

Zhang Shuo¹, Zhu Pengfei ¹, Fan Hao¹& Liu Zhenxia¹

¹School of Power and Energy, Northwestern Polytechnical University

Abstract

The external gear pump is an important component of the aero-engine lubricating oil system. When the aero-engine is starting, due to the combined effects of the relative positions between the oil tank and the pump, the internal leakage of the pump, and the downstream flow resistance, the air inside the oil suction pipe will enter the external gear pump. Then the air will circulate in the pump and cannot be emitted. This phenomenon is the airlock. To fully analyze the mechanism of the airlock of the external gear pump, based on several typical starting conditions of a certain type of gear pump, the computational fluid dynamics software Pumplinx4.6.0 was used to simulate the airlock phenomenon. The mechanism of the airlock was obtained. A numerical calculation method for airlock analysis was established and verified by an experiment. The results show that (1) The airlock of the gear pump is mainly caused by the air trapped in the pump and the suction pipe, the excessive downstream flow resistance, the radius, and end face clearances;(2) The gear pump's ability to pressurize the air is very limited at the airlock state and the air cannot overcome the resistance downstream the pump; (3) There is an internal circulation flow(the upstream area of the pump -gear cavity- the downstream area of the pump -clearance- the upstream area of the pump) in the pump at the airlock state; (4) With the gear pump rotational speed increasing, the pressurizing ability of the pump increases and the outlet pressure at the airlock state increases.

Keywords: external gear pump, airlock, internal leakage, CFD, experimental study

1. Introduction

The external gear pump is the core component of the oil supply stage in the aero-engine lubricating oil system. During the engine starting process, there are various influencing factors such as the relative height between the oil tank and the oil pump, internal leakage of the pump clearance, and flow resistance in the pipeline. [1] These factors can cause air to enter the lubricating oil system and circulate in the pump, which is known as air-lock. This situation can lead to pressure loss in the lubricating oil system, oil supply failure, and serious engine malfunctions.

The internal flow system of the engine, such as the fuel system and the lubricating oil system, may experience an airlock during operation. This phenomenon is closely related to the air stored in the pipeline. Early research on the airlock phenomenon began in the 1930s. N. F. SCUDDER et al. studied the airlock problem of the fuel system of the piston propeller engine. They used the whole machine test method to study the operating temperature of different positions in the fuel system and the boiling temperature of different aviation fuels. They also studied changing the pipeline design and equipping the vapor separator to solve the airlock problem. [2] PIGOTT discussed the design of the fuel system of cars, including the fuel tank and the fuel supply pump. He proposed that the fuel vapor precipitation produces heterogeneous fluids which the meter is unable to measure, and summarized the calculation methods of the maximum tank temperature and the maximum altitude. [3] J.K. Pearson et al. developed a mathematical model to simulate airlock phenomenon. The model can be used to predict the engine performance of different fuels at different temperatures, and can also predict the impact of component changes in the engine fuel system. The model's predictive ability for automotive fuel systems was verified by experiments. [4] Kitae Yeom et al. took piston engines as the research object and conducted experimental research to solve the problem of airlock during fuel injection. The fuel of this engine is liquefied petroleum gas, which is easy to vaporize. They proposed a high-pressure fuel pipe to prevent the airlock phenomenon. [5] Li Guoquan et al.

took an external gear pump as the research object and explained the principle of airlock formation based on the CFD method. They used FLUENT software to simulate the airlock phenomenon and obtained the airlock characteristics of gear pumps at different rotational speeds and different teeth widths. This model is highly simplified and the working fluid is air. [6] K Thanikasalam et al. reviewed the potential risk of airlock in aero-engines using gasoline. They concluded that the designers of the fuel system of aircraft engines must fully consider the influence of fuel characteristics, mechanical vibration, engine heat, and environmental conditions. [7] Ananth Manickam Wash et al. proposed a prediction model for the possibility of airlock formation in the fuel system of piston aero-engines, and used this model to evaluate 14 types of aviation fuels. The airlock formation of various fuels at multiple working conditions was obtained, and the experimental results were in good agreement. [8] As the most commonly used pump in the oil supply system, the research on external gear pumps is relatively abundant. Farhad Sedri et al. conducted numerical simulation and experimental research on an external gear pump. To solve the problem of large radial leakage of gear pumps under high pressure, a method to machine a shallow groove on the gear teeth surface was proposed. This structure can effectively reduce pressure pulsation and leakage. [9] Alessandro Corvaglia et al. used Pumplinx software to calculate an external gear pump to study the flux fluctuation at the outlet of an external gear pump. The pressure fluctuation data by the numerical calculation model was consistent with the experimental results. [10]. Paulina Szwemin et al. researched the radial and axial clearance leakage problems of external gear pumps using the CFD method. The numerical calculation model of the external gear pump was established using FLUENT software. They analyzed the influence of gear shaft eccentricity on internal leakage and pressure distribution on the outer circumferential surface. [11] Alessandro Corvaglia et al. studied the problems of incomplete filling and cavitation of liquid on the suction side of an external gear pump. They used Pumplinx software to calculate helical and spur gear pumps and conducted experimental studies. The experimental results were consistent with the numerical results. [12] To simplify the internal flow analysis of external gear pumps, Alexander Mitov et al. developed a simplified two-dimensional numerical calculation model of external gear pumps using CFX software. The numerical results of this calculation model were verified by other experimental research results.[13]

It can be seen that research on external gear pumps is mainly focused on structural optimization and normal internal flow state, and the purpose of the research is to improve the flow characteristics. For the airlock phenomenon, the research object is often the fuel system. The working fluid is vaporized fuel. There is little research on the airlock state of the gear pump in the lubricating oil system. The fluid used in the existing research is single-phase air, and there is a lack of research on the airlock phenomenon of two-phase flow under actual conditions.

Given the above shortcomings, this paper builds the oil supply part of the lubricating oil system and simulates the airlock state of the external gear pump by adjusting the outlet pressure and rotational speed. This paper uses Pumplinx4.6.0 software to perform transient calculations on external gear pumps and combines experimental methods to study its airlock flow characteristics under two-phase flow conditions.

2. Numerical methods and experimental set

2.1 Geometric structure

The object is an external gear pump (Figure 1) used in the lubricating oil system of an aero-engine. The inlet pipe diameter is 30 mm, and the outlet cross section is approximately a rectangle of 20*29 mm. The gear parameters are shown in Table 1. Based on the geometric structure of this gear pump, numerical calculations and experimental studies are carried out at various conditions.

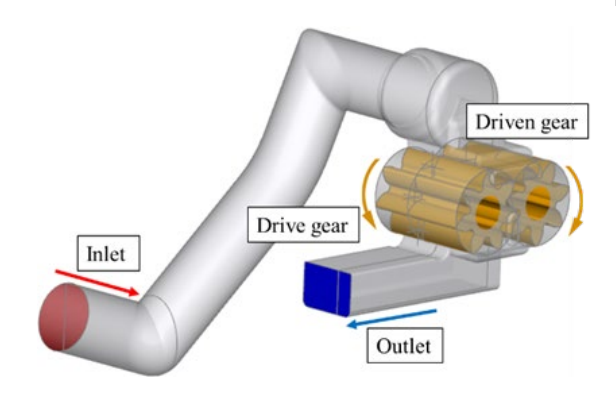


Figure 1 – External gear pump.

Table 1 – Geometric parameters.

rabie i Geemetrie parametere:		
	Module	4
	Number of teeth	7
Gear	Teeth width (mm)	50
	Tip clearance (mm)	0.04-0.114
	End-face clearance (mm)	0.05-0.134

2.2 Numerical method

This study includes two special flow phenomena. First, the cavitation phenomenon occurs at the separation point of the gear pump at normal operating conditions. This paper uses the Singhal full cavitation model to simulate the cavitation phenomenon. The model has been verified by experiments and proved to be able to simulate the cavitation phenomenon of the gear pump. [14]

Second, the airlock occurs during the starting process of the gear pump. This paper introduces the volume of fluid method (VOF) to simulate the airlock phenomenon. Since the working fluid inside the gear teeth cavity is air when the airlock occurs, the oil stays in the suction pipe of the pump, so there is an obvious two-phase interface. This two-phase flow state is suitable for the application of the VOF method [15]. This method can effectively capture the two-phase interface.

Considering that the fluid in the teeth cavity area is irritated by the gears and the flow state is fully developed turbulence, the RNG k-epsilon turbulence model is used for calculation.

Figure 2 shows the mesh structure. This paper uses CFD software Pumplinx4.6.0 for numerical simulation. The inlet and outlet pipeline areas are divided into orthogonal grids, and the gear area is divided into structured grids. The interface connecting the two volumes is connected by a mismatched grid interface (MGI). This connection method does not require the mesh to have common nodes on the interface. The mesh density is adjusted according to the calculation conditions, and the wall mesh is refined to ensure that the y+ value is within a reasonable range. The total amount of mesh is about 780,000.

Here, the mesh size is described in detail. Since the internal flow field of the pump suction pipe and the pump rear pipeline is relatively uniform, the maximum mesh scale is set to 0.02mm and the minimum is 0.0008mm in these two volumes, and the wall mesh scale is set to 0.005mm. A cylindrical density body is set near the gear meshing area (Figure 2). The radius of this area is 17mm, and the mesh scale in the area is limited to 0.004mm. The transition of the mesh scale is realized by setting this density body. A structured grid is divided in the gear teeth cavity area, with 360 units in the circumferential direction, 8 units in the radial direction, and 12 units in the axial direction.

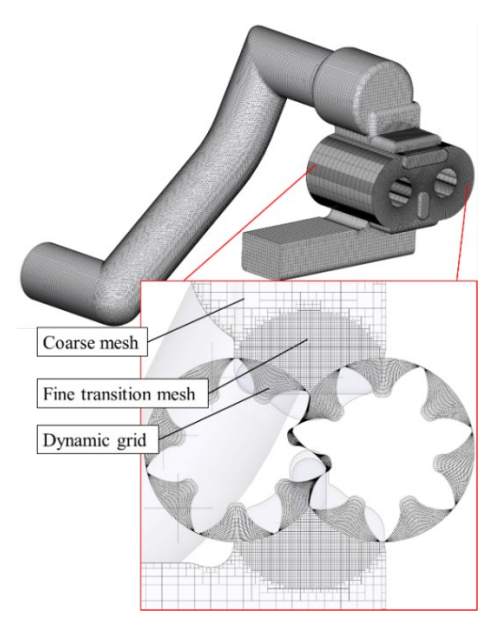


Figure 2 – Mesh structure.

The boundary conditions of the two flow states involved in the calculation are shown in Table 2. The lubricating oil system uses a suction-type oil supply method, and the internal pressure of the oil tank is atmospheric. The outlet of the fluid domain is set as a pressure outlet. At normal conditions, the outlet pressure value is determined by experiment. At airlock conditions, the outlet pressure value is obtained by assuming and trial calculation. The remaining boundaries are set as no-slip walls.

Table 2 – Boundary conditions.

Table 2 Bearlady conditions.				
	Normal	Airlock		
Inlet	Static pressure (101kPa)	Static pressure (101kPa)		
Outlet	Static pressure (experimental data)	Static pressure (trial calculation)		
Working fluid	Oil	Air(initial fluid) Oil(inlet)		

According to the actual working conditions, the gear pump rotational speed range is determined to be 400-1000r/min. The lubricating oil physical parameters are shown in Table 3.

Table 3 – Oil physical parameters.

Temperature	Density	Dynamic viscosity
(°C)	(g/cm3)	(Pa·s)
24	0.9720	0.0477

Here we explain the trial calculation method of the airlock condition. The fluid inside the flow field is air, and the fluid at the inlet part is lubricating oil. As shown in Figure 3, in the initial flow field, there is a volume of lubricating oil at the inlet (the yellow translucent volume in the figure), and the rest of the volume is filled with air.

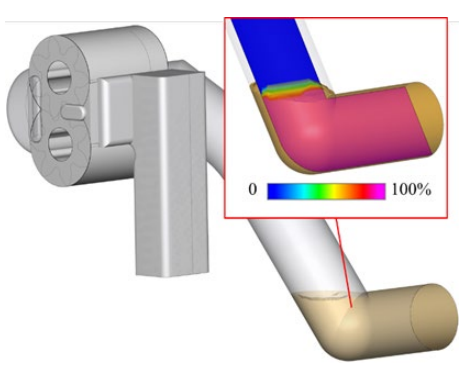


Figure 3 – Initial fluid field.

Assuming that the outlet pressure is a certain value, after calculating for a while, the change in oil volume and air flux of the outlet are obtained. As shown in Figure 4, when the outlet pressure is set to a small value (a), the lubricating oil in the inlet section gradually expands downstream, and the outlet air flow is positive. When the outlet pressure is set to a large value (c), the lubricating oil in the inlet section gradually flows back until it disappears, and the outlet air flow is negative. When the outlet pressure makes the flow just in the airlock state (b), the lubricating oil volume in the inlet section is unchanged, and the outlet air flow is approximately 0.



Figure 4 – Different oil volumes at the inlet.

2.3 Experimental set

The experimental system of this study is mainly composed of an oil supply system, gas supply system, experimental part, pressure stabilizer, power system, oil return system, and test system. The principle of the experiment is shown in Figure 5. The oil supply system provides sufficient clean lubricating oil for the experimental parts. The air supply system provides pressurized air for the pressure stabilizing chamber to maintain the required constant pressure inside. The experimental part is an external gear pump. The inlet of the pump is connected to the fuel tank. The outlet of the pump is divided into two parts, which are used to supply lubricating oil to different positions of the aero-engine. Transparent observation sections are installed in these three parts of the pipeline to monitor the flow. The pressure stabilizing chamber is used to provide stable pressure downstream. It is equipped with a pressure sensor and a vent valve for monitoring and regulating internal pressure. The power system provides rotational power. The oil return system is used to pump the lubricating oil from the scavenge tank back to the oil tank to ensure the circulation of the system. The monitoring data are rotational speed, pressure of the stabilizing chamber, pressure downstream of the pump, and outlet flow rate.

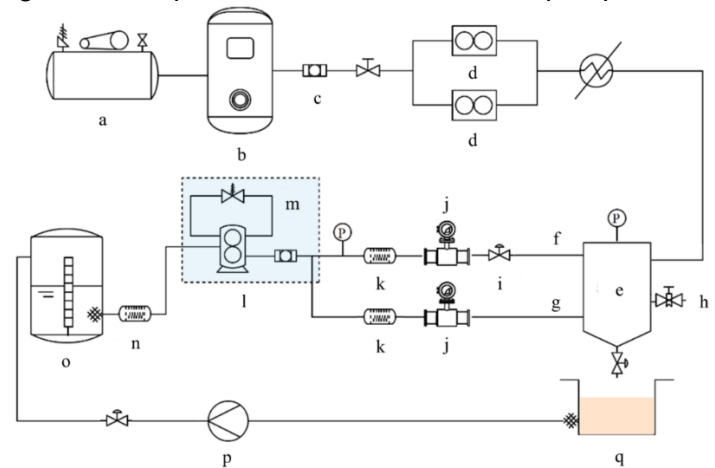


Figure 5 – Experimental set.

(a) Air compressor (b) Air storage tank (c) Air filter (d) Flowmeter (e) Pressure stabilizing chamber (f) Outlet 1 (g) Outlet 2 (h) Vent valve (i) Regulating valve (j) Flowmeter (k) Transparent observation section (l) Lubricating oil pump (m) Pressure regulating valve (n) Transparent observation section (o) Oil tank (p) Oil return pump (q) Scavenge tank

3. Result analysis

3.1 Airlock mechanism analysis

The schematic diagram of the oil supply principle of the lubricating oil system is shown in Figure 6. The main components of this structure are the lubricating oil tank, the oil suction pipe, and the external gear pump. The connection between the oil suction pipe and the lubricating oil tank is located at a low position of the oil tank, and the pump is located at a higher position. In the figure, h_1 is the internal height of the lubricating oil tank, h_2 is the liquid level, and h_3 & h_4 are the heights of the lowest and highest positions of the oil suction pipe.

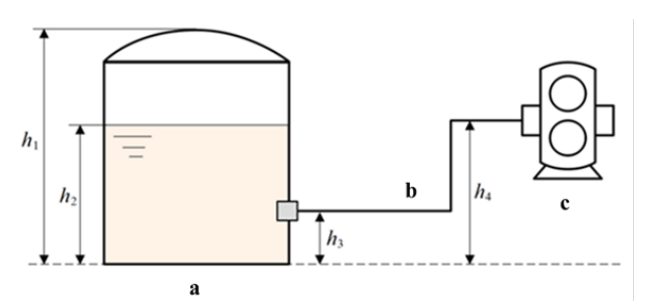


Figure 6 – Oil supply system.

The occurrence of the problem of oil supply failure caused by the airlock of the gear pump during the starting process is closely related to the following factors:

- (1) The oil tank is located at a low position or there is an upward-mounted oil pipe. The presence of air in the oil suction pipe between the oil tank and the gear pump is a necessary condition for the airlock. After the lubrication system starts, especially during the first start (when there is no lubrication oil inside the pipe and pump), the working fluid inside is air. Since air is much more compressible than lubricating oil, the pressure downstream of the pump is smaller at the same rotational speed.
- (2) The flow resistance of the downstream pipe, oil filter, valve, nozzle, and other structures and components downstream of the pump is too large. The pressurized air in the pump cannot pass through the above structures.
- (3) For external gear pumps, there are multiple structural clearances. Among them, the end-face clearance and the tip clearance are the main ways for internal leakage. After the gear pump pressurizes the air, there is a pressure gradient from the back to the front of the pump. Therefore, with this pressure gradient, the air tends to flow along the above two structural gaps to the front of the pump with smaller flow resistance.

3.2 Typical normal conditions

This section selects the normal working condition with a rotational speed of 500r/min for flow field characteristic analysis. As shown in Figure 7, the gear pump has a significant pressurization effect on the lubricating oil. There is a pressure gradient in the flow field along the direction of the red arrow in the figure. It should be noted that the maximum pressure position in the flow field appears in the area where the gears are about to mesh, that is, the position marked with No. 1 in the figure. This area is the oil-trapped area of the external gear pump. The lowest pressure position in the flow field appears in the area where the gear meshing is about to separate, that is, the position marked with No. 2 in the figure.

During the operation of the gear pump, the oil enters the gear teeth cavity and is transported downstream. In this process, a part of the oil will be sucked into the gear meshing area. With the meshing process, this part of the oil is strongly squeezed by the gears, and the pressure rises sharply. Most of the oil enters the pump through the unloading groove on the gear pump shell, and a small part of it remains in the area between the teeth top and the teeth root of another gear and enters the front of the pump. When the meshing part begins to separate, the space suddenly increases, and the pressure in this part of the volume drops sharply. When the pressure drops below the saturated vapor pressure of the lubricating oil at this temperature, the lubricating oil begins to vaporize, which is called cavitation. As can be seen from the mark No. 2 in the figure, the cavitation area is approximately the same as the low-pressure area.

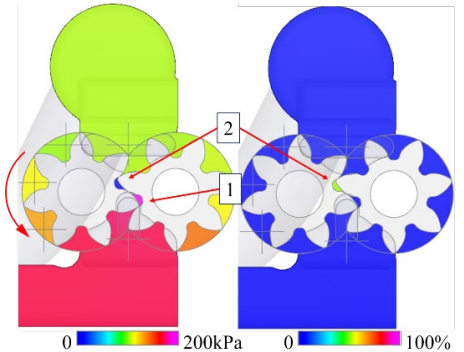


Figure 7 – Static pressure and vapor distributions.

As shown in Figure 8, the flow field section is intercepted at the position of half the teeth width. Due

INSERT RUNNING TITLE HERE

to the rotation of the gear, the fluid in the teeth cavity has a flow velocity. When the fluid carried by the teeth cavity of the two gears collides, it can be seen from the figure that a high-velocity area appears. As the fluid flows to the outlet, the velocity distribution of the flow field after the pump gradually becomes uniform.

From the local flow velocity vector diagram, it can be seen that the flow direction of the fluid inside the teeth cavity is the same as the direction of the gear linear velocity. There is no obvious leakage flow in the tip clearance.

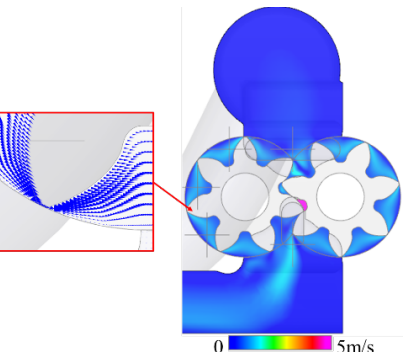


Figure 8 – Velocity magnitude distributions and vectors.

As shown in Figure 9, the gear meshing causes the oil flow velocity between the trapped oil area and the unloading groove to be higher.

From the local flow velocity vector diagram, it can be seen that there is a certain reverse leakage flow in the end-face clearance. This part is end-face leakage. However, under normal working conditions where the fluid is oil, the leakage is small. In summary, it can be seen that under normal working conditions, the main flow path inside the gear pump is a one-way flow: the upstream area of the pump -the gear cavity- the downstream area of the pump.

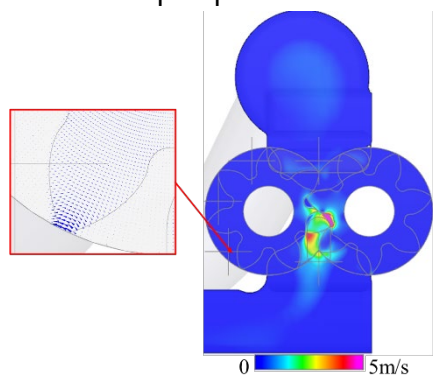


Figure 9 – Velocity magnitude distributions and vectors (end-face).

3.3 Typical airlock conditions

This section selects the working condition of 500r/min for flow field characteristics analysis. Using the trial calculation method introduced in Section 2.2, the outlet pressure of the airlock state at this rotational speed is 2.7kPa. To compare the impact of the change of working fluid on the pressurizing capacity of the gear pump, five pressure sampling points at the half-teeth width section position are selected as shown in Figure 10.

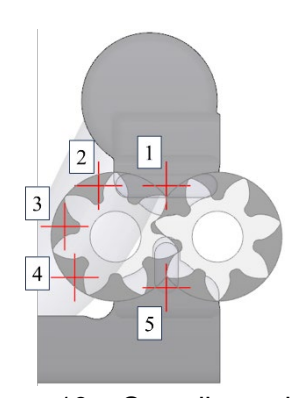


Figure 10 – Sampling points.

INSERT RUNNING TITLE HERE

As shown in Figure 11, the pressure distribution of the normal working condition is compared with that of the airlock condition. At point No.1, the pressure of both conditions is atmospheric. Starting from No. 3, the pressure of the normal working condition begins to be significantly greater than the pressure of the airlock condition. At the downstream area of the pump, under normal conditions, the gear pump has pressurized the lubricating oil from atmospheric pressure to 168kPa. While under the airlock condition, the gear pump can only pressurize the internal air to 104kPa, which is much less than the former. The gear pump is a pressurizing component of the lubricating oil system, and the pressurization of the air cannot overcome the flow resistance of the downstream pipeline. At this time, an airlock will occur.

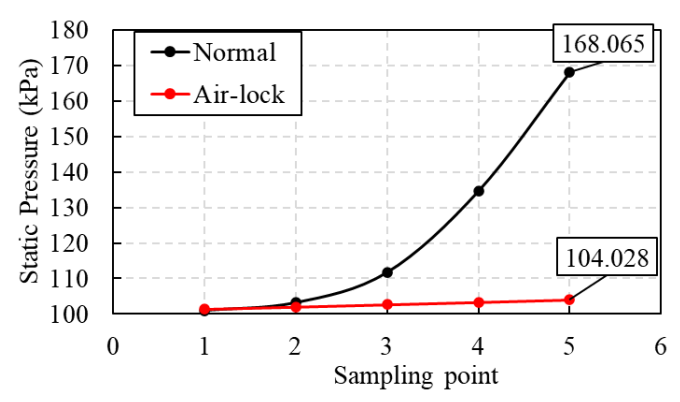


Figure 11 – Circumferential pressure distribution.

As shown in Figure 12, when the working fluid is air, there is a pressure gradient in the flow field along the direction of the red arrow in the figure. This pressure gradient is much smaller than the pressure gradient when the working fluid is lubricating oil. The air pressure gradually rises in the direction indicated by the arrow in the figure and reaches the highest point at the downstream area of the pump. Since the lubricating oil is not sucked into the teeth cavity area, there is no cavitation phenomenon. Due to the low viscosity and strong fluidity of air, there is no local pressure increase in the meshing area.

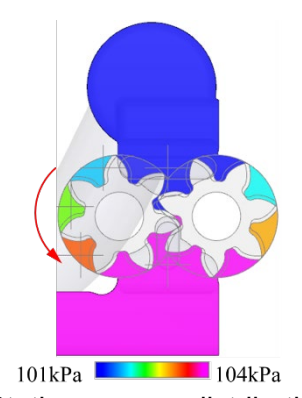


Figure 12 – Static pressure distributions (airlock).

As shown in Figure 13, due to the rotation of the gear, the fluid inside the teeth cavity close to the teeth surface is of a high flow velocity. Under the airlock condition, there is an area with a higher flow velocity near the inside of the gear pump housing, and the fluid in this area flows along the wall. It can be seen from the local flow velocity vector diagram that the flow direction of this part of the fluid is opposite to the flow direction of the fluid inside the teeth cavity. Driven by the pressure gradient between different teeth cavities, the fluid in the tip clearance area flows from the high-pressure area to the low-pressure area, forming an obvious tip leakage phenomenon.

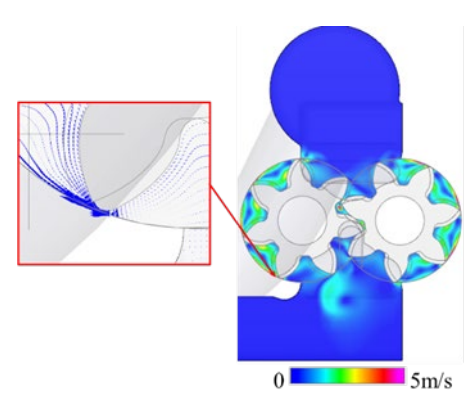


Figure 13 – Velocity magnitude distributions and vectors (airlock).

As shown in Figure 14, the area with a higher velocity is similar to the gear teeth shape. Since the flow cross-sectional area of the end face clearance is small, the same flow rate of airflow has a higher velocity when flowing through the clearance. It can be seen from the local flow velocity vector diagram that, under the effect of the pressure gradient between adjacent teeth cavities, the air flows from the high-pressure area to the low-pressure area through the end-face cclearance, forming an obvious end-face leakage phenomenon.

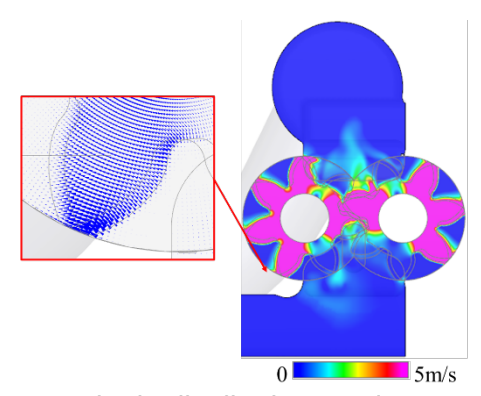


Figure 14 – Velocity magnitude distributions and vectors (end face, airlock).

The calculation results of different rotational speeds are shown in Figure 15. As the pump outlet pressure increases, the outlet air flux gradually decreases to 0. When the flow rate is 0, the gear pump is in the airlock state. The outlet pressure of the airlock state and rotational speed are positively correlated.

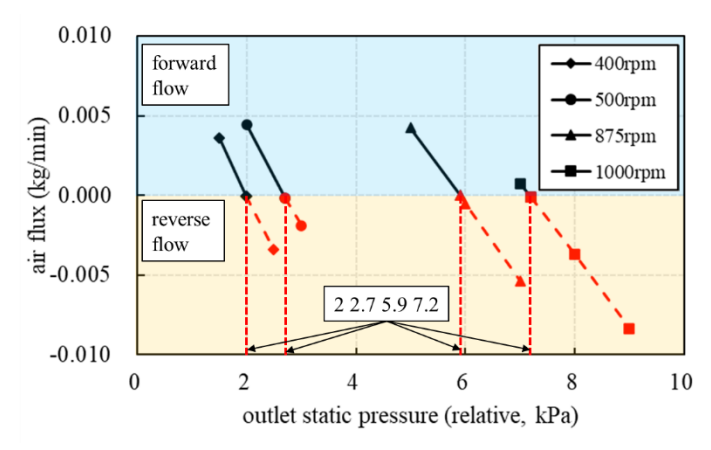


Figure 15 – Outlet pressure at different rotational speeds (airlock).

Figure 16 shows that the pressure distribution in the area between the gear surface and the shell surface in the non-meshing area is uneven. The pressure gradually increases along the direction of gear rotation.

INSERT RUNNING TITLE HERE

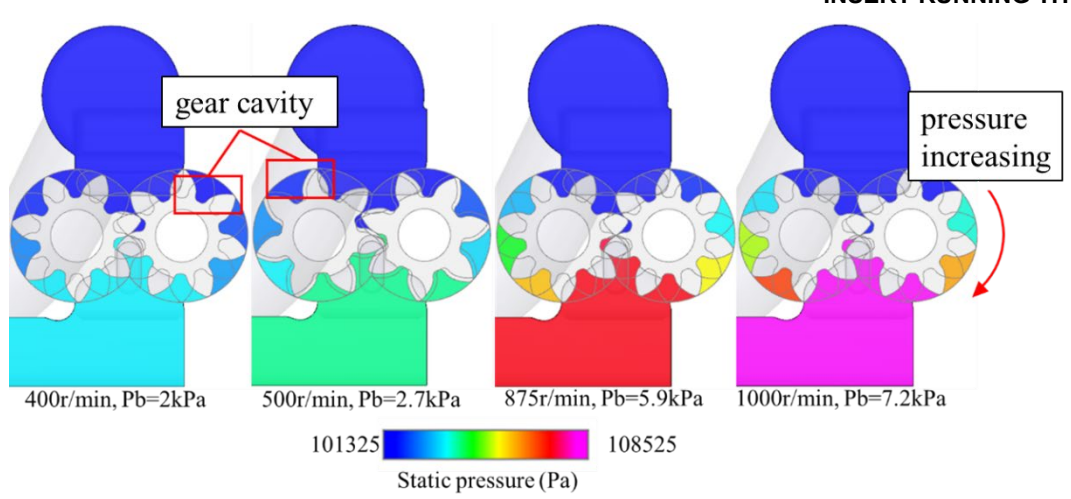


Figure 16 – Static pressure distributions at different rotational speeds (airlock).

Figures 17 and 18 show that:

- (1) There is an airflow generated by the rotation of the gear inside the teeth cavity, and the speed is positively correlated with gear rotational speed, while the airflow speed at the outlet is 0.
- (2) There is a high-speed flow driven by the pressure gradient between adjacent teeth cavities at the tip clearance, that is, tip leakage.
- (3) The flow speed in the end-face clearance area is high.

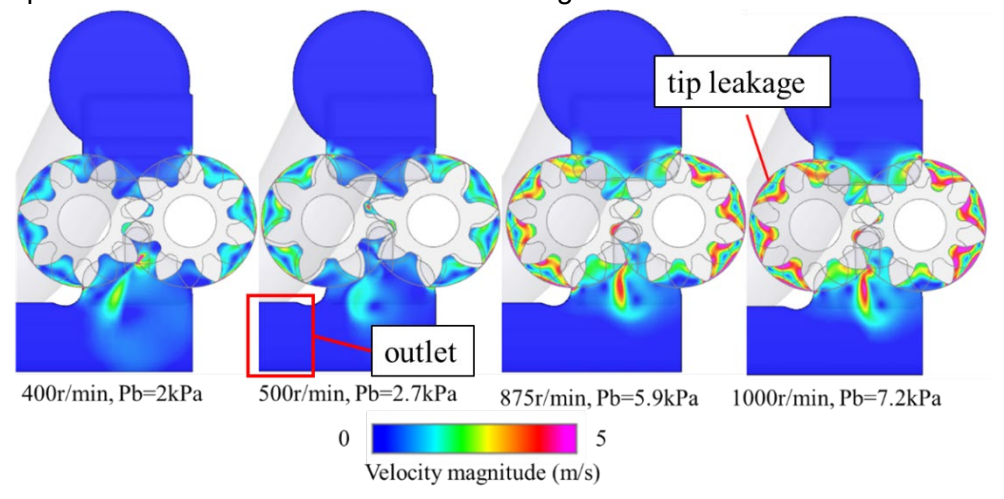


Figure 17 – Velocity magnitude distributions at different rotational speeds (airlock).

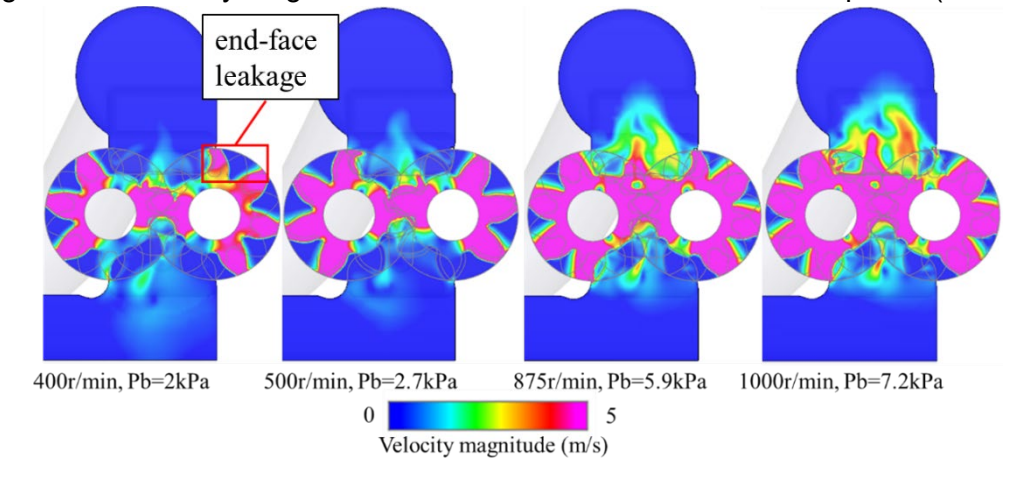


Figure 18 – Velocity magnitude distributions at different rotational speeds (end-face airlock).

3.4 Experimental results

The gear pump experiment under normal working conditions is carried out. Figure 19 is a comparison between the computational and the experimental values of the outlet oil flux. When the rotational speed is 200r/min, the pressurization of the lubricating oil is very limited. The value measured by the

pressure sensor is less than 10% of the sensor range, and the system error is large. At this time, the relative deviation between the computational result (the boundary condition is based on the measured data) and the experimental result is about 10%. When the rotational speed is higher than 200r/min, the relative deviation is reduced to less than 7%.

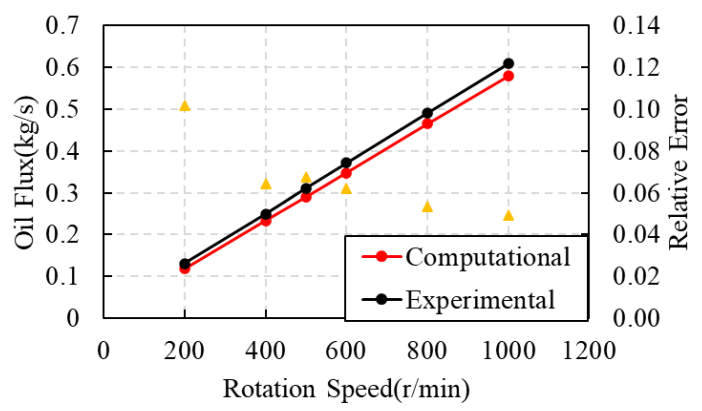


Figure 19 – Comparison between computational and experimental results (normal).

The test was carried out under the airlock state when the inlet fluid was pure oil and the inside of the pump was air. Normally, its end-face clearance and tip clearance are within a certain range (Table 1). However, the clearance parameters of the actual external gear pump are difficult to determine. So the airlock pressure should be between the airlock pressure value corresponding to the maximum clearance and the airlock pressure value corresponding to the minimum clearance.

Figure 20 is a comparison of the airlock pressure experimental and the computational value at different rotational speeds. Under all conditions, the test values are between the maximum calculated value and the minimum calculated value, and the trend of change with the rotational speed is the same. It can be seen that the established numerical calculation method can effectively determine the upper and lower limits of the outlet pressure when airlock occurs in the lubricating oil pump.

In summary, the numerical method used in this study can accurately simulate the working state of the external gear pump at the airlock state.

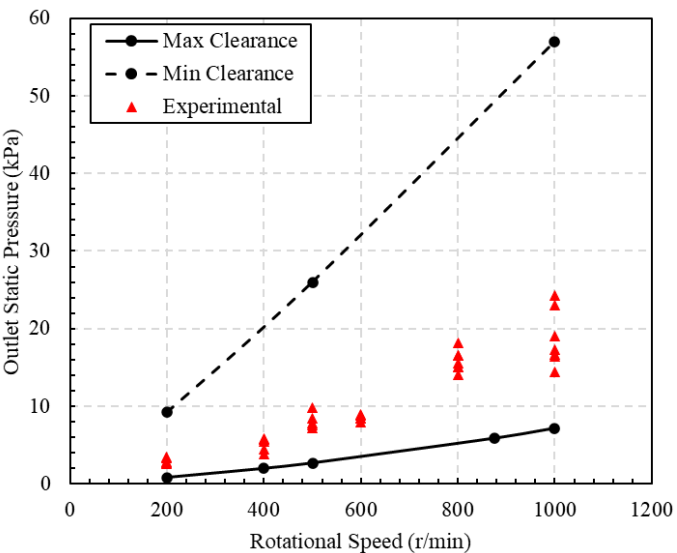


Figure 20 – Comparison between computational and experimental results (airlock).

A detailed analysis of the experimental data of the airlock state at 500r/min shows that:

- (1) There is no flow in the high-pressure range (yellow background). At this time, the internal fluid of the gear pump is air, and the high post-pump pressure prevents the air from being discharged.
- (2) When the outlet pressure drops to around 8.5kPa, the gear pump is still in the airlock state. After the pressure drops slightly, the pump quickly sucks the lubricating oil and then runs stably.
- (3) The airlock critical pressure obtained from four repeated experiments is in the range of 7.2kPa to 8.5kPa.
- (4) After the outlet pressure drops to less than the airlock critical pressure, the oil flow rate is independent of the outlet pressure.

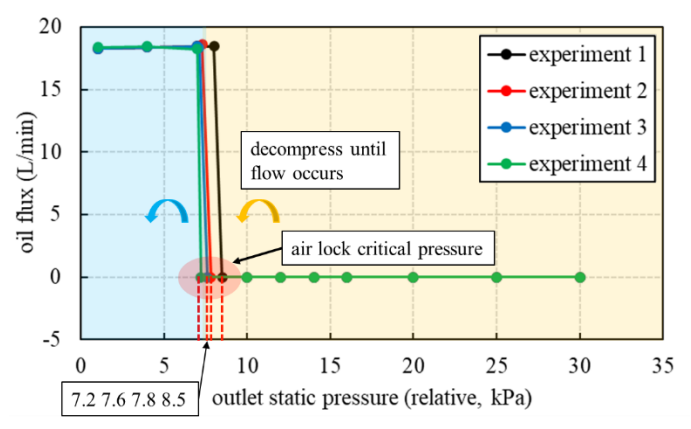


Figure 21 – Experimental result of 500r/min.

4. Discussions and conclusions

This paper analyzes the structure of the oil supply part of the aircraft engine lubricating oil system and obtains the conditions for the occurrence of the airlock. Taking a certain type of oil supply external gear pump as the research object, the mechanism of airlock is analyzed, and a numerical calculation method for airlock analysis is formed. The reliability of the numerical method is verified by experiments. The normal working conditions and airlock working conditions are calculated, and the internal flow field is compared and analyzed. The internal flow characteristics of the external gear pump under the airlock state are obtained. It provides a theoretical basis and a reliable numerical method for the design of airlock prevention of the lubricating oil system.

Based on the analysis of the numerical and experimental results, the conclusions are as follows:

- (1) The airlock phenomenon is related to three conditions: the low initial oil level of the lubricating oil tank, the existence of air in the upstream pipeline of the pump (necessary condition), the flow resistance created by the downstream components, and the end-face clearance and tip clearance in the gear pump.
- (2) When the airlock occurs in the gear pump, the fluid in the pump has reverse leakage flow at the tip clearance and the end-face clearance. The wall-adherent reverse flow occurs on the outer wall of the gear cavity. The fluid in each gear cavity is driven by the gear and transferred from the upstream of the pump to the downstream side. The flow direction is the same as the gear linear speed direction.
- (3) With the increase of pump rotational speed, the outlet pressure of the airlock status increases. The numerical results show that when the speed of the pump increases from 400r/min to 1000r/min, the relative pressure at the pump outlet increases from 2kPa to 7.2kPa under the airlock status.
- (4) The experimental results show that when the outlet pressure is less than the critical pressure of the airlock, the pump sucks the lubricating oil instantly and reaches the stable operation state quickly. The steady flow rate is a fixed value, which has no obvious correlation with the outlet pressure.

5. Contact Author Email Address

Mail to: zhupengfei@nwpu.edu.cn

6. Copyright Statement

The authors confirm that they, and/or their company or organization, hold copyright on all of the original material included in this paper. The authors also confirm that they have obtained permission, from the copyright holder of any third party material included in this paper, to publish it as part of their paper. The authors confirm that they give permission, or have obtained permission from the copyright holder of this paper, for the publication and distribution of this paper as part of the ICAS proceedings or as individual off-prints from the proceedings.

7. ACKNOWLEDGEMENTS

This work was supported by the National Science and Technology Major Project (J2019-III-0023-0067) In China.

Reference

- [1] Liu Z, and Jiang P. Mechanical System Design of Aero-engines, Science Press, 2022
- [2] Scudder, N. F. Flight Test Research on the Problem of Vapor Lock. Journal of the Aeronautical Sciences, Vol. 6, No. 2, pp 68-71, 1938.
- [3] Pigott. Vapor Lock-or Dumb Engineering. SAE Technical Paper, No. 440180, 1944.
- [4] Pearson, J K, Caddock B D and Orman P L. A Computer Model for the Prediction of Vapor Lock in the Fuel Pump of a Carburetted Engine. SAE Technical Paper, No. 821201, 1982.
- [5] Yeom K, Park J, Bae C, Park J and Kim S.. Anti-vapor lock of a top-feed injector for a liquefied petroleum gas liquid-phase injection engine. Energy & fuels, Vol. 23, No. 2, pp 876-883, 2009.
- [6] Li G and Huang J. Aeroengine Oil Pump Airlock Preventive Methods. Aeroengine, Vol. 37, No. 1, pp 1-3, 2011.
- [7] Thanikasalam K, Rahmat M, Fahmi A M, Zulkifli A M, Shawal N N, Ilanchelvi K and Elayarasan R. IOP Conf. Series: Materials Science and Engineering. International Conference on Aerospace and Mechanical Engineering, Malaysia, Vol. 370, No. 1, 012008, 2018.
- [8] Wash A M, Kumar T, Mohsin R, Majid Z A and Ghafir, M. F. A. Application of factor analysis in the determination of vapor lock tendency in aviation gasolines/motor gasoline/blends and the compatibility as alternatives in naturally aspirated aviation engines. Alexandria Engineering Journal, Vol. 60, No. 6, pp 5703-5724, 2021.
- [9] Sedri F and Riasi A. Investigation of leakage within an external gear pump with new decompression slots: numerical and experimental study. Journal of the Brazilian Society of Mechanical Sciences and Engineering, Vol. 41, pp 1-12, 2019.
- [10] Corvaglia A, Ferrari A, Rundo M and Vento O. Three-dimensional model of an external gear pump with an experimental evaluation of the flow ripple. Proceedings of the Institution of Mechanical Engineers, Part C: Journal of Mechanical Engineering Science, Vol. 235, No. 6, pp 1097-1105, 2021.
- [11] Szwemin P and Fiebig W. The influence of radial and axial gaps on volumetric efficiency of external gear pumps. Energies, Vol. 14, No. 15, pp 4468, 2021.
- [12] Corvaglia A, Rundo M, Bonati S and Rigosi M. Simulation and experimental activity for the evaluation of the filling capability in external gear pumps. Fluids, Vol. 8, No. 9, pp 251, 2023.
- [13] Mitov A, Nikolov N, Nedelchev K and Kralov I. CFD Modeling and Experimental Validation of the Flow Processes of an External Gear Pump. Processes, Vol. 12, No. 2, pp 261, 2024.
- [14] Singhal AK, Athavale MM, Li H, and Jiang Y. Mathematical basis and validation of the full cavitation model. Fluids Eng. Vol. 124, No. 3, 2002.
- [15] Hirt CW and Nichols BD. Volume of fluid (VOF) method for the dynamics of free boundaries. Journal of computational physics. Vol. 39, No. 1, 1981.